

LAP SHEAR TEST OF A MAGNESIUM FRICTION SPOT JOINT: NUMERIC MODELING

Leonardo Contri Campanelli ¹
Armando Ítalo Sette Antonialli ²
Nelson Guedes de Alcântara ³
Claudemiro Bolfarini ⁴
Uceu Fuad Hasan Suhuddin ⁵
Jorge Fernandez dos Santos ⁶

Abstract

Friction spot welding (FSpW) is one of the most recently developed solid state joining technologies. In this work, based on former publications, a computer aided draft and engineering resource is used to model a FSpW joint on AZ31 magnesium alloy sheets and subsequently submit the assembly to a typical shear test loading, using a linear elastic model, in order to conceive mechanical tests results. Finite element analysis shows that the plastic flow is concentrated on the welded zone periphery where yield strength is reached. It is supposed that “through the weld” and “circumferential pull-out” variants should be the main failure behaviors, although mechanical testing may provide other types of fracture due to metallurgical features.

Key words: Friction welding; Magnesium; Finite element; Shear test.

ENSAIO DE CISALHAMENTO EM UMA JUNTA POR FRICÇÃO POR PONTO DE MAGNÉSIO: MODELAGEM NUMÉRICA

Resumo

A soldagem por fricção por ponto (FSpW) é uma das tecnologias desenvolvidas mais recentemente no que se refere à união no estado sólido. Neste trabalho, com base em publicações anteriores, é utilizado um recurso computacional de desenho e projeto para modelar uma junta por FSpW em chapas de liga de magnésio AZ31 e, posteriormente, submeter o conjunto a uma carga de cisalhamento típica, usando um modelo elástico linear, a fim de compreender os resultados dos ensaios mecânicos. A análise por elementos finitos mostra que o escoamento plástico concentra-se na periferia da zona soldada onde a tensão limite de escoamento é atingida. Presume-se que as variantes “através da solda” e “arrancamento circunferencial” sejam os principais modos de falha, ainda que os ensaios mecânicos venham a apresentar outros tipos de fratura em razão de fatores metalúrgicos.

Palavras-chave: Soldagem por fricção; Magnésio; Elementos finitos; Ensaio de cisalhamento.

¹Materials Engineer, MSc. Student of Graduate Program on Materials Science and Engineering, Federal University of Sao Carlos – UFSCar, Rod. Washington Luiz, km 235, Cep 13565-905, São Carlos, SP, Brazil. E-mail: leocampa@hotmail.com

²Mechanical Engineer, MSc. PhD Student of Graduate Program on Materials Science and Engineering, Federal University of Sao Carlos – UFSCar, Rod. Washington Luiz, km 235, Cep 13565-905, São Carlos, SP, Brazil. E-mail: antonialli@ufscar.br

³Materials Engineer, PhD, Associate Professor at Department of Materials Engineering, Federal University of Sao Carlos – UFSCar, Rod. Washington Luiz, km 235, Cep 13565-905, São Carlos, SP, Brazil. E-mail: nelsong@ufscar.br

⁴Materials Engineer, PhD, Titular Professor at Department of Materials Engineering, Federal University of Sao Carlos – UFSCar, Rod. Washington Luiz, km 235, Cep 13565-905, São Carlos, SP, Brazil. E-mail: cbolfa@ufscar.br

⁵Metallurgical Engineer, PhD, Scientist at Department of Solid State Joining Processes, Institute of Materials Research, Helmholtz-Zentrum Geesthacht – HZG, Max-Planck-St. 1, D-21502 Geesthacht, Germany. E-mail: uceu.suhuddin@hzg.de

⁶Metallurgical Engineer, PhD, Head of Department of Solid State Joining Processes, Institute of Materials Research, Helmholtz-Zentrum Geesthacht – HZG, Max-Planck-St. 1, D-21502 Geesthacht, Germany. E-mail: jorge.dos.santos@hzg.de

I INTRODUCTION

Friction based joining techniques derived from friction stir welding (FSW) have increased the interest of automotive and aircraft industries due to the advantages over the conventional fusion processes, including the possibility of joining dissimilar and non-weldable materials such as highly alloyed 2XXX and 7XXX aluminum series. With the welding procedure being conducted in the solid state, the main restrictions associated to the metal solidification (e.g. hot cracking, porosity and splash) are fully avoided and the intrinsic lower energy input reduces the distortion of the workpiece and the microstructural changes.⁽¹⁾ One of the most recent techniques, friction spot welding (FSpW) employs an especially designed non-consumable tool (consisting of pin, sleeve and clamping ring) to produce a spot connection between overlapped similar/dissimilar sheets through frictional heat and plastic deformation.⁽²⁾ Figure 1 shows a schematic illustration of the four typical steps resulting from the independent motion of each tool component in “sleeve plunge variant”.

Basically, while clamping ring fixes the overlapped sheets against an anvil, the plunging and rotating component (either pin or sleeve) generates frictional heat and softens the surrounding material, which flows to create a solid state bond between the upper and lower sheets. FSpW was developed to reduce the limitations of consolidated techniques currently applied in the spot joining of structural components in the transportation sector, such as weight penalty, high consumable costs and corrosion problems in mechanical fastening (clinching, riveting and self-piercing riveting)⁽³⁾ or defects associated to material melting and solidification in fusion welding processes (resistance and laser spot welding).^(4,5) Friction spot connections exhibit good surface finishing and, as far as there is low material loss, no keyhole is left on the surface at the end of the joining operation, contrary to friction stir spot welding (FSSW) process. As soon as the mechanical performance of FSpW joints is demonstrated to be at least similar, the process may be capable of replacing the mentioned techniques in some applications.

Analytical and numerical modeling has been increasingly applied as an effort to better comprehend the friction spot joining mechanisms. Muci-Küchler, Kalagara and Arbegast⁽⁶⁾ developed a thermo-mechanical finite element model (FEM) in Abaqus/Explicit software to calculate the temperature distribution and plastic deformation of a refill FSSW process. FEM was also used by Li and Kang⁽⁷⁾ to evaluate the thermal field in FSSW joints of AM60B magnesium alloy performed with different combinations of parameters. In case of Hirasawa et al.,⁽⁸⁾ besides the evaluation of temperature distribution, the material flow resulting from different FSSW tool geometries is analyzed by means of an elastic-plastic deformation model using the particle method. Kim et al.⁽⁹⁾ evaluate the performance of FSSW aluminum joints through the development of a FEM in PAM-Crash software to predict the effect of distinct tool geometries on weld strength, and a finite volume method (FVM) in STAR-CD software to analyze the material flow patterns around the tool and therefore explain the considerable different strengths achieved among the tool geometries.

Mazzaferro et al.⁽¹⁰⁾ originally extend the referred efforts to FSpW technique in order to comprehend the joint mechanical behavior and failure modes, including the effect of the morphology and properties of each welding region. Different numerical models are developed in SolidWorks and Abaqus software to reproduce both the specimen geometry and the load conditions in lap shear and cross tensile mechanical tests. Experimental results and simulations exhibit a satisfactory compatibility, with similarities in the levels of stresses and the specimen distortions.

In this way, the purpose of this work is to develop some simple finite element models of an AZ31 magnesium alloy friction spot joint, considering only linear elastic behavior, and verify the stresses distribution in the vicinity of the weld nugget subjected to a typical tensile shear loading, thus helping the assessment of the different resulting failure behaviors.

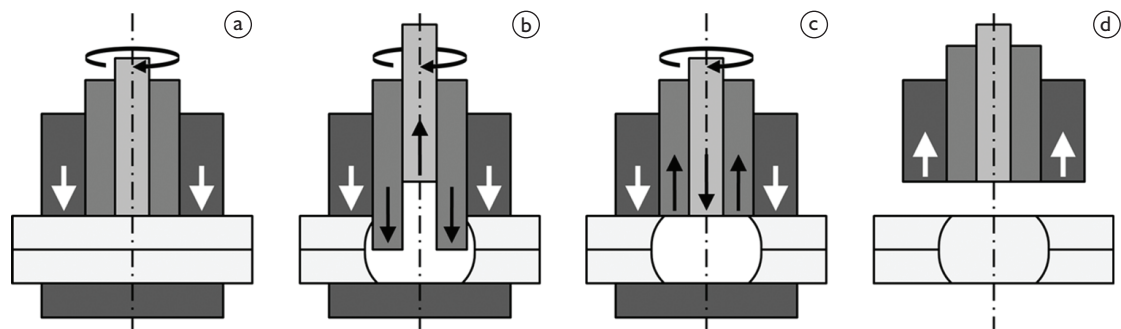


Figure 1. Illustration of “sleeve plunge variant” stages: (a) clamping and tool rotation; (b) sleeve plunge and pin retraction; (c) parts back to surface level; and (d) tool removal.

2 MATERIAL AND METHODS

In former works developed by the authors,^(11,12) lap shear tests were carried out in order to discuss the effect of some important welding parameters like rotational speed, plunge depth and dwell time over the resistance of a FSpW joint. Microstructural examination on the cross-sections of the welded joints provides the identification of three different zones: base material (BM), thermo-mechanically affected zone (TMAZ) and stir zone (SZ), besides the hook at the interface of the overlapped sheets. Nonetheless, microhardness profile (Figure 2) presents no pronounced variation along the welded joint.

Face to that, it was decided to explore geometric modeling of the welded joint to apply on the finite element analysis (FEA) of a typical lap shear test, so that failure behaviors of the specimens could be predicted or even explained. The approach considers the distinction of the weld nugget and the presence of the hook, and then

four different models are proposed, according to Figure 3: indistinct weld nugget without hook (model I), indistinct weld nugget with hook (model II), distinct weld nugget without hook (model III) and distinct weld nugget with hook (model IV).

Both bending and vertical displacement of the extremity of the interface between the sheets in the models containing hook are intentionally magnified in order to intensify the effect of the hook over the mechanical performance. In the models without hook, the flat extremity of the interface is representative of the insignificant vertical displacement of the defect. Using CosmosWorks[®], a couple of AZ31 magnesium alloy sheets (2 mm thick, 60 mm wide and 138 mm long) joined by a 9 mm friction spot weld on the middle of the 46 mm overlap (dimensions according to ISO 14273:2000 standard)⁽¹³⁾ is subjected to a 5 kN shearing load, value about the ultimate force measured on the real test (Figure 4).

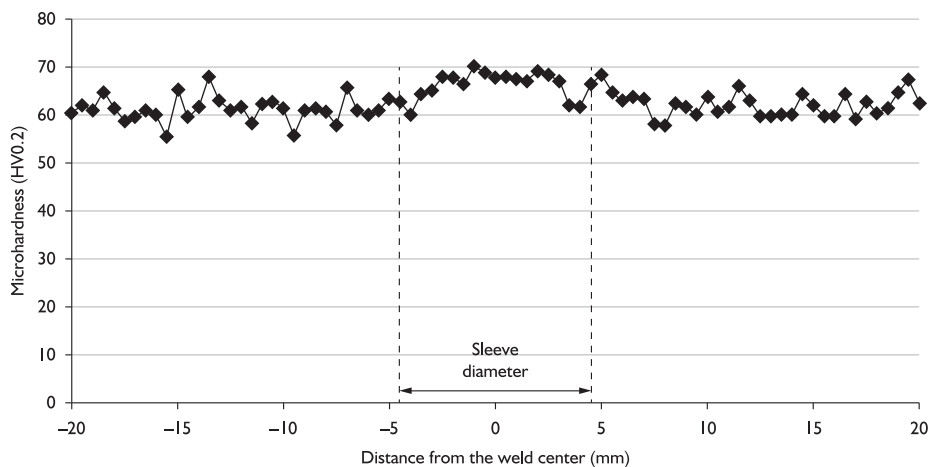


Figure 2. Typical microhardness profile at the cross section of the joint.⁽¹¹⁾

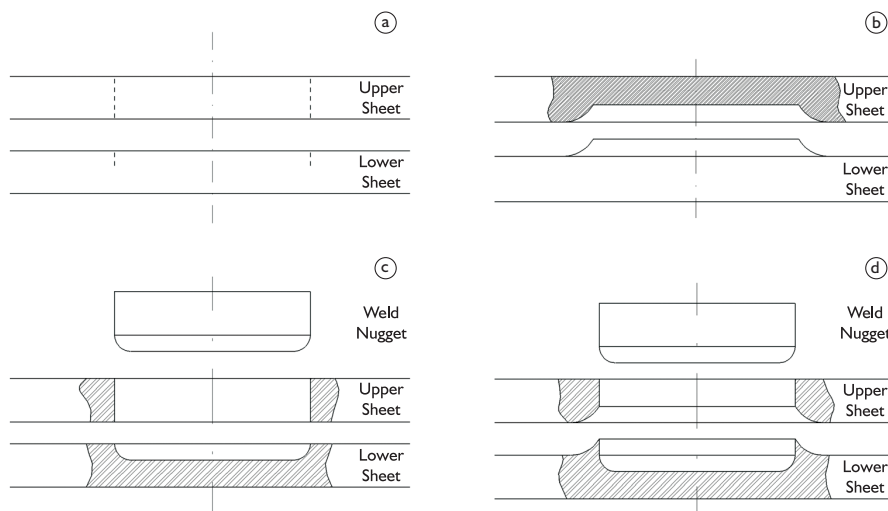


Figure 3. Different geometric features of the welded joint: (a) model I, (b) model II, (c) model III and (d) model IV.

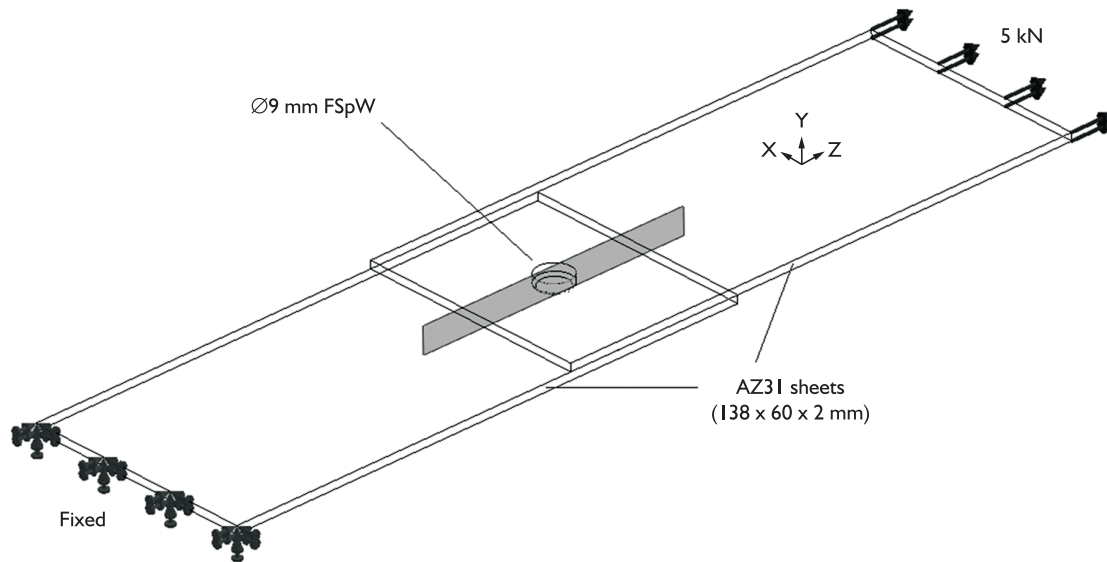


Figure 4. Shear test assembly for finite element analysis.

As no significant difference of hardness is found between BM, TMAZ and SZ (Figure 2)⁽¹¹⁾, both sheets and the weld nugget (on models III and IV) are modeled as an isotropic linear elastic material with the same yield strength. Table I presents elastic modulus (E), Poisson ratio (ν) and yield strength (σ_y) of the AZ31B-H24 magnesium alloy adopted in the simulation. Considering that this alloy presents low ductility, this simple linear elastic model is not too far away from its real behavior.

Contact between sheets, on models I and II, and between each sheet and the weld nugget, on models III and IV, is set as bonded and restricted to the spot weld boundary (not on the hook). H-adaptative meshes were generated using nearly 600,000 parabolic tetrahedral elements, which originated about 400,000 nodes for each model. From generalized Hooke's Law (Equation 1)⁽¹⁴⁾ it is possible to correlate the stresses state of each node of the mesh discretized in the FEA model with the corresponding strain state, obtained from nodal displacement. Note that S_x , S_y and S_z mean normal stress while τ_{yz} , τ_{zx} and τ_{xy} mean shear stress; on the other hand, ϵ_x , ϵ_y and ϵ_z are linear strains whilst γ_{yz} , γ_{zx} and γ_{xy} are angular strains.

$$\begin{Bmatrix} S_x \\ S_y \\ S_z \\ \tau_{yz} \\ \tau_{zx} \\ \tau_{xy} \end{Bmatrix} = \frac{E}{(1+\nu)(1-2\nu)} \begin{bmatrix} 1-\nu & \nu & \nu & 0 & 0 & 0 \\ \nu & 1-\nu & \nu & 0 & 0 & 0 \\ \nu & \nu & 1-\nu & 0 & 0 & 0 \\ 0 & 0 & 0 & \frac{1-2\nu}{2} & 0 & 0 \\ 0 & 0 & 0 & 0 & \frac{1-2\nu}{2} & 0 \\ 0 & 0 & 0 & 0 & 0 & \frac{1-2\nu}{2} \end{bmatrix} \begin{Bmatrix} \epsilon_x \\ \epsilon_y \\ \epsilon_z \\ \gamma_{yz} \\ \gamma_{zx} \\ \gamma_{xy} \end{Bmatrix} \quad (1)$$

Table I. Mechanical properties of AZ31 magnesium alloy⁽¹⁵⁾

Alloy	E (GPa)	ν	σ_y (MPa)
AZ31B-H24	45	0.35	220

3 RESULTS AND DISCUSSIONS

Figure 5 shows the z-normal stress distribution around the spot joint during lap shear test for the models previously introduced (Figure 3). The surfaces illustrated correspond to the transverse cutting plane parallel to the loading direction (see gray colored plane on Figure 4), where the highest tensile and compressive stresses are identified.

Considering the distinction of the weld nugget, a comparison between models I and III illustrates that the stresses distribution is similar for both cases, that is, tensile stress in the loaded side (right side) of the upper sheet and in the clamped side (left side) of the lower one. In the presence of hook, however, the distribution around the joint presents some particularities in model IV in comparison to model II. The existence of a distinct weld nugget promotes the extension of both tensile and compressive regions along the curvature of the nugget base. Regarding the occurrence of the hook, the presence of the defect slightly changes the stresses distribution on the upper sheet. The tensile and compressive regions above the interface between the overlapped sheets are concentrated on the tip of hook pattern. Moreover, the stresses are fully intensified at the top surface.

Plastic flow must initiate in the regions subjected to the highest tensile stresses, which are located below the extremity of the interface in the clamped side and above the extremity in the loaded side, when the yield strength is reached. Specifically for models I and III, independently of the distinction of the weld nugget, fracture may propagate

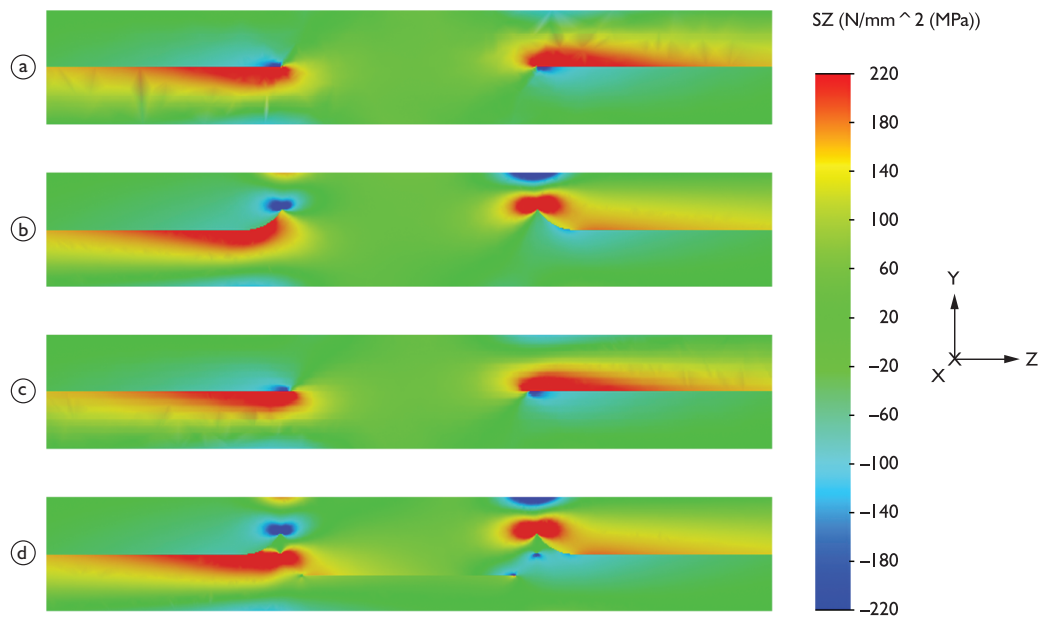


Figure 5. Stresses distribution around the spot joint for: (a) model I, (b) model II, (c) model III and (d) model IV.

through the welded zone following the tensile stresses until the complete separation of the joint, although it is possible that propagation initially occurs through the external surface of the sheet in both sides until a compressive zone is reached. The mentioned fracture behavior is known as “through the weld” (TW) mode and is possible for all simulated models, but it is the unique for the models that contemplate absence of hook.

For models II and IV, two different crack propagation paths are possible. Failure originated in the clamped side tends to get away from the compressive zone in the tip of hook region. Therefore, crack may propagate through the welded region or around the zone under compression towards the tensile stressed region at the top surface and then surrounding the welded joint. For the fracture nucleated in the loaded side, crack starts propagating perpendicularly to the surface. Since a compressive zone is observed near the surface of the upper sheet, the failure front may stop extending. In this case, crack may be reached by the crack growing through the welded region to completely separate the joint (TW mode). However, if the opposite failure propagation happened surrounding the welded region, less effort is required for the loaded side crack to propagate through the region under compression and therefore the weld nugget is entirely removed from the joint. Such fracture behavior is designated “circumferential pull-out” (CPO) mode.

As previously mentioned, model IV presents some particularities related to the extension of both tensile and compressive regions along the curvature of the nugget base. In this case, crack nucleated in the clamped side may propagate initially towards the surface of the lower sheet

following the tensile stressed extension. Continuing with the propagation, failure may proceed to the region under high tensile stresses in the loaded side where the crack already existing is reached. The described fracture behavior can also be pointed out as a particular TW mode.

4 CONCLUSIONS

Finite element analysis can be successfully applied on conceiving the fracture behavior of friction spot joints submitted to lap shear loading. Each proposed geometric model is useful to predict the different failure paths. According to that, plastic flow is concentrated in the vicinity of the welded zone where tensile stresses reach the highest values, inducing permanent damage. Crack propagation is therefore expected to proceed through the welded zone, resulting on the complete collapse of the joint (“through the weld” variant). Otherwise, crack would flow around the weld nugget boundary, inducing its detachment (“circumferential pull-out” variant). Other fracture behavior modes may only be ascribed to metallurgical features, which cannot be considered on a linear elastic approach.

Acknowledgements

The authors acknowledge the financial support provided by FAPESP (Sao Paulo Research Foundation) and CNPq (National Council for Scientific and Technological Development), Brazil.

REFERENCES

- 1 Mishra RS, Ma ZY. Friction stir welding and processing. *Mater Sci Eng Reports*. 2005;50:1-78. <http://dx.doi.org/10.1016/j.mser.2005.07.001>
- 2 Schilling C, Santos J, inventores; GKSS – Forschungszentrum Geesthacht, produtor. Method and device for linking at least two adjoining work pieces by friction welding. United States patent US 6,722,556 B2. 20 abr. 2004.
- 3 Barnes TA, Pashby IR. Joining techniques for aluminium spaceframes used in automobiles. Part II: adhesive bonding and mechanical fasteners. *J Mater Process Tech*. 2000;99:72-9. [http://dx.doi.org/10.1016/S0924-0136\(99\)00361-1](http://dx.doi.org/10.1016/S0924-0136(99)00361-1)
- 4 Briskham P, Blundell N, Han L, Hewitt R, Young K. Comparison of self-pierce riveting, resistance spot welding and spot friction joining for aluminium automotive sheet. Warrendale: SAE International; 2006. (SAE technical paper, 2006-01-0774).
- 5 Yang YS, Lee SH. A study on the joining strength of laser spot welding for automotive applications. *J Mater Process Tech*. 1999;94:151-6. [http://dx.doi.org/10.1016/S0924-0136\(99\)00094-1](http://dx.doi.org/10.1016/S0924-0136(99)00094-1)
- 6 Muci-Küchler KH, Kalagara S, Arbegast WJ. Simulation of a refill friction stir spot welding process using a fully coupled thermo-mechanical FEM model. *J Manuf Sci Eng*. 2010;132:014503. <http://dx.doi.org/10.1115/1.4000881>
- 7 Li B, Kang HT. Temperature distribution during friction stir spot welding of magnesium alloy AM60B. *J Test Eval*. 2011;39:16-24. <http://dx.doi.org/10.1520/JTE101910>
- 8 Hirasawa S, Badarinarayan H, Okamoto K, Tomimura T, Kawanami T. Analysis of effect of tool geometry on plastic flow during friction stir spot welding using particle method. *J Mater Process Tech*. 2010;210:1455-63. <http://dx.doi.org/10.1016/j.jmatprotec.2010.04.003>
- 9 Kim D, Badarinarayan H, Ryu I, Kim JH, Kim C, Okamoto K et al. Numerical simulation of friction stir spot welding process for aluminum alloys. *Met Mater Int*. 2010;16:323-32. <http://dx.doi.org/10.1007/s12540-010-0425-9>
- 10 Mazzaferro JAE, Rosendo TS, Mazzaferro CCP, Ramos FD, Tier MAD, Strohaecker TR et al. Preliminary study on the mechanical behavior of friction spot welds. *Soldagem Insp*. 2009;14:238-47. <http://dx.doi.org/10.4028/www.scientific.net/MSF.706-709.3016>
- 11 Campanelli LC, Suhuddin UFH, Santos JF, Alcantara NG. Preliminary investigation on friction spot welding of AZ31 magnesium alloy. *Mat Sci Forum*. 2012;706-709:3016-3021. <http://dx.doi.org/10.4028/www.scientific.net/MSF.706-709.3016> <http://dx.doi.org/10.1016/j.jmatprotec.2012.11.002>
- 12 Campanelli LC, Suhuddin UFH, Antonialli AIS, Santos JF, Alcântara NG, Bolfarini C. Metallurgy and mechanical performance of AZ31 magnesium alloy friction spot welds. *J Mater Process Tech*. 2013;213:515-521. <http://dx.doi.org/10.1016/j.jmatprotec.2012.11.002>
- 13 International Organization of Standardization. ISO 14273:2000: Specimen dimensions and procedure for shear testing resistance spot, seam and embossed projection welds. Geneva; 2000.
- 14 Bathe K-J. Finite element procedures. New Jersey: Prentice Hall; 1996.
- 15 Housh S, Mikucki B. Properties of magnesium alloys. In: American for Metals. Properties and selection: nonferrous alloys and special-purpose materials. Materials Park: ASM International; 1990. v. 2, p. 480-516.

Recebido em: 17/10/2012

Aceito em: 15/02/2013